Supporting Information

Preparation and Application of Flexible Conductive Organohydrogels with Ultrahigh Gas-permeability

Jianhua Wang[a], Zifeng Ding[a], Jinhao Yang[b], Jing Cheng[a], Chenguang Huang[a], Caihua Xiong[b], Xixi Cai[a], Lijun You[a, *], Shaoyun Wang[a, *]

[a]College of Biological Science and Engineering, Fuzhou University, Fuzhou, 350108, China

[b]School of Mechanical Science & Engineering, Huazhong University of Science and Technology, Wuhan 430074, China

*Corresponding author: Lijun You; Shaoyun Wang

Phone: +86-591-22866375; fax: +86-591-22866278

E-mail address: ibptylj@fzu.edu.cn (L. You); shywang@fzu.edu.cn (S. Wang)

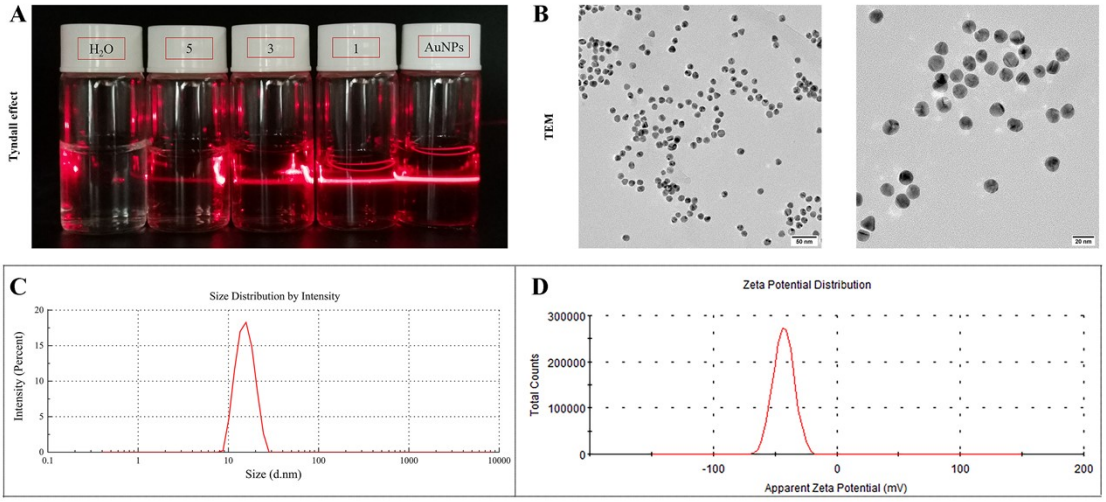

Fig. S1. (A) The AuNPs dispersion prepared has the Tyndall effect and the number represents the dilution multiple of the original solution. (B) TEM, (C) particle size, and (D) zeta potential of AuNPs.

Note: A bright 'pathway' can be observed from the vertical direction of the incident light (Fig. S1A). AuNPs prepared by the sodium citrate reduction method had the Tyndall effect. The particle size and potential were characterized, and the average particle size was 14.87 nm (Fig. S1C), which might be wrapped with water, and the PDI was 0.140. The potential is -43.0 Mv (Fig. S1D). It indicated that the prepared gold nanoparticles had good morphology, uniform particle size distribution, and strong stability. The concentration was 10.64 nmol/L.

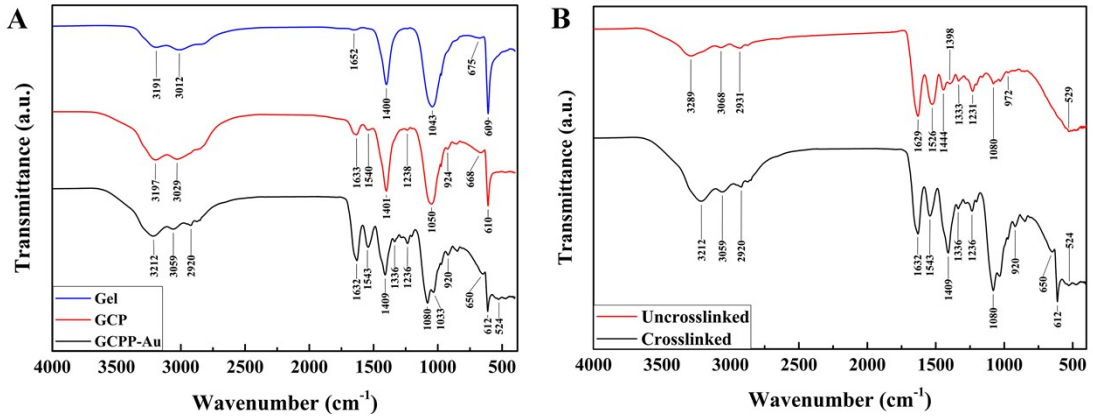

Fig. S2. FT-IR spectrogram of (A) Gel/GCP/GCPP-Au conductive organohydrogels and (B) GCPP-Au conductive gel before and after crosslinking.

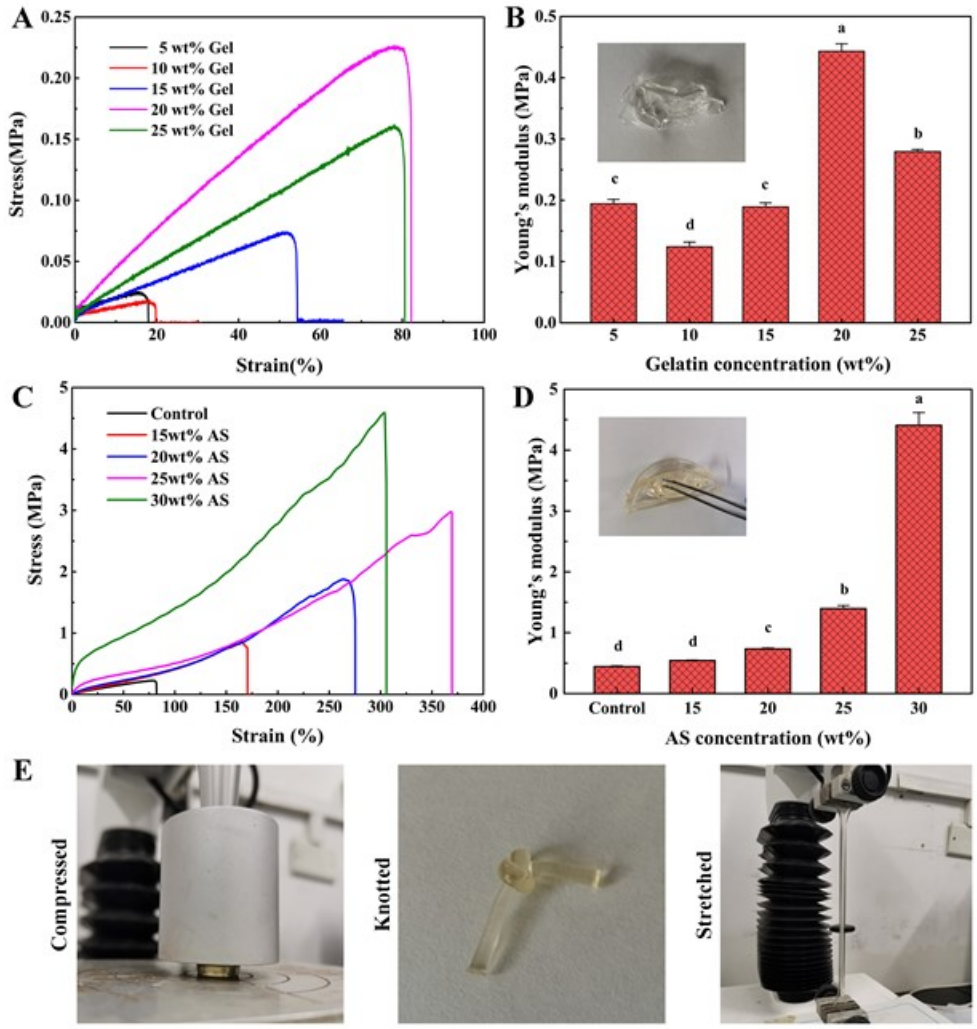

Fig. S3. (A) Compressive stress-strain curves different concentrations of gelatin hydrogels, (B) unsoaked AS solutions, and (C) Young's modulus of different concentrations of gelatin hydrogels. (D) Compression stress-strain Curve of 20 wt% gelatin hydrogel immersed in different concentrations of AS solutions, (E) soaked AS solutions, (F) young's modulus of 20 wt% gelatin hydrogel immersed in different concentrations of AS solutions. (G) Gelatin hydrogels were compressed, knotted, and stretched after soaking in AS solutions. Relevant statistical significance is denoted by differing letters ($p<0.05$).

Note: It can be seen that the mechanical strength was high when the gelatin concentration was 20wt% (Fig. S3A & B). However, it was still fragile under the action of external forces because of high water content usually accompanied by weak mechanical properties. Studies have found that AS has the Hofmeister effect on gelatin hydrogel to achieve toughening [1]. Therefore, gelatin-ammonium sulfate hydrogel was prepared by soaking gelation in AS solutions with different concentrations. The results showed that the mechanical properties of the hydrogel were significantly improved. When AS was 25wt%, the elongation at break reached 370%, increasing by 4.5 times (Fig. S3C & D). The mechanical properties were enhanced after soaking AS, which could be compressed, knotted, and stretched (Fig. S3E).

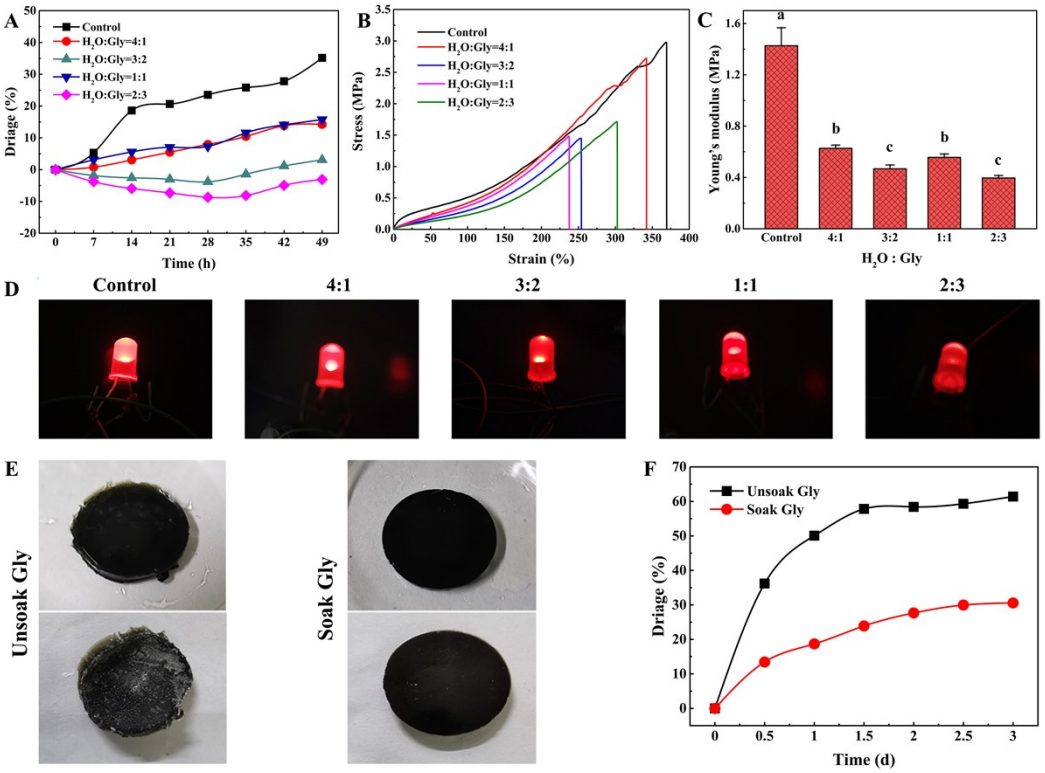

Fig. S4. Moisture retention property of conductive organohydrogels. (A) Driage, (B) Tensile stress-strain curves, and (C) young's modulus, statistical significance is denoted by differing letters ($p<0.05$). (D) Luminescence of diodes of gelatin hydrogel immersed in different Gly concentrations. (E) Changes and (F) driageof GCPP-Au conductive gel after 3 days of storage.

Note: From Fig. S4A, the moisture retention performance of gelatin hydrogels was significantly improved after adding Gly into AS solution. The higher the proportion of Gly, the stronger the moisture retention performance, but the mechanical properties were also significantly reduced (Fig. S4B & C), and the brightness of the diode was also weakened (Fig. S4D), which indicated that the Gly would also affect the electrochemical performance. Further verification was carried out in GCPP-Au, and when the solvent of AS solution was added with Gly, no serious water loss and salt analysis were observed in the material (Fig. 3E), and the driage was reduced to 30% (Fig. S4F).

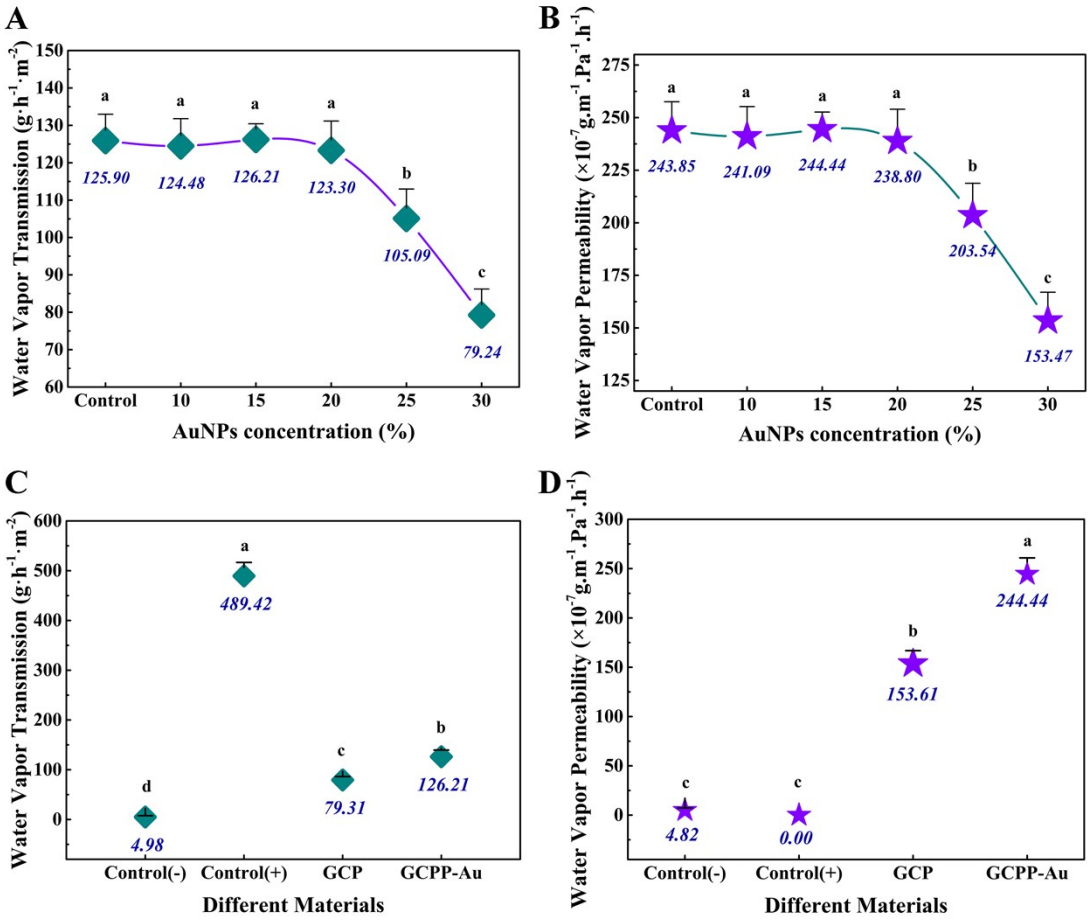

Fig. S5. (A) Water vapor permeability (WVT) and (B) Water vapor permeability (WVP) coefficient of GCPP-Au conductive Gels. WVT (C) and WVP (D) of different materials. Statistical significance is denoted by differing letters ($p < 0.05$).

Note: The GCP, GCPP-Au conductive organohydrogels, and preservative film (negative control) were covered on the sample bottle and compared with the sample bottle in an open state (positive control). It was found that the WVT of GCPP-Au was 25 times higher than that of negative control (4.98 $g \cdot h^{-1} \cdot m^{-2}$) and 1.6 times higher than that of GCP (79.31 $g \cdot h^{-1} \cdot m^{-2}$) (Fig. S4 C), and the WVP of GCPP-Au was much higher than that of negative control ($4.82 \times 10^{-7} g \cdot m^{-1} \cdot Pa^{-1} \cdot h^{-1}$) and GCP group ($153.61 \times 10^{-7} g \cdot m^{-1} \cdot Pa^{-1} \cdot h^{-1}$) (Fig. S4 D).

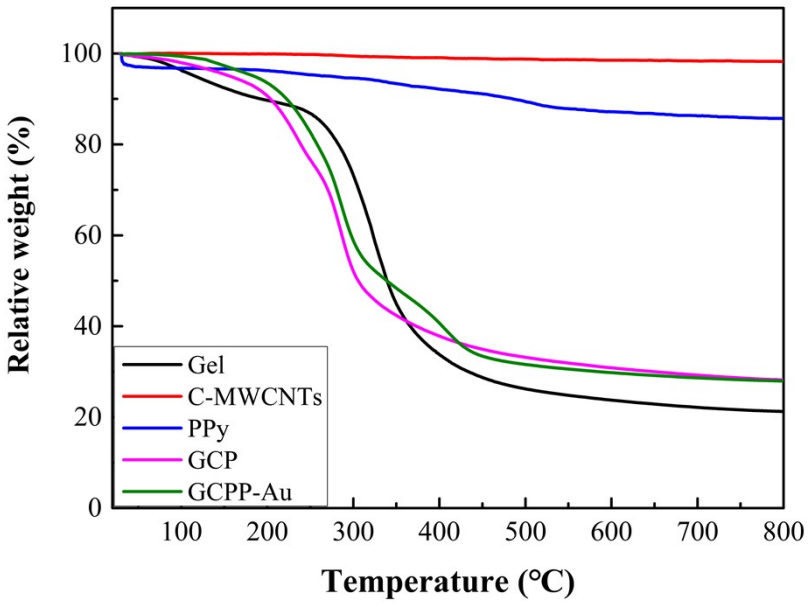

Figure S6. Thermogravimetric (TGA) curves of gelatin, C-MWCNTs, PPy, GCP, and GCPP-Au conductive organohydrogels

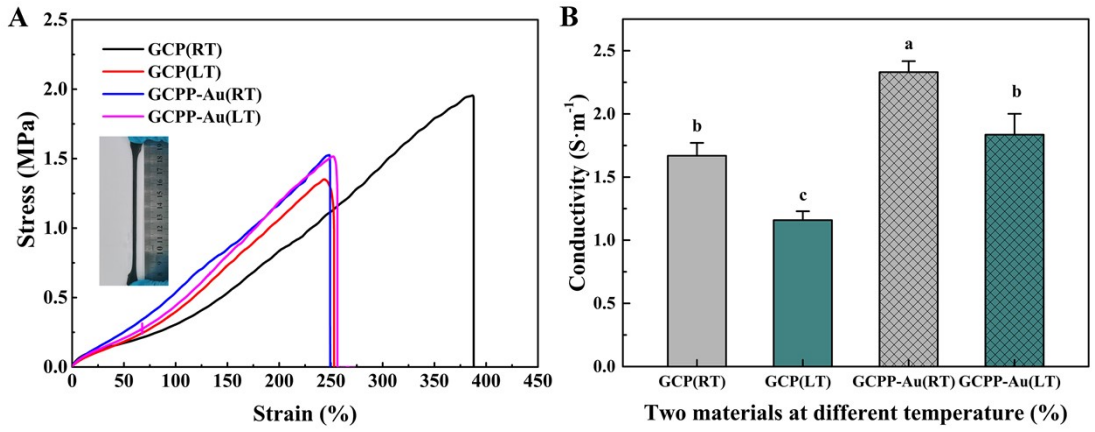

Fig. S7. (A) The tensile stress-strain curve and (B) conductivity change diagram of GCP and GCPP-Au conductive organohydrogels after low-temperature (-35℃) storage for 24 hours. Relevant statistical significance is denoted by differing letters ($p<0.05$).

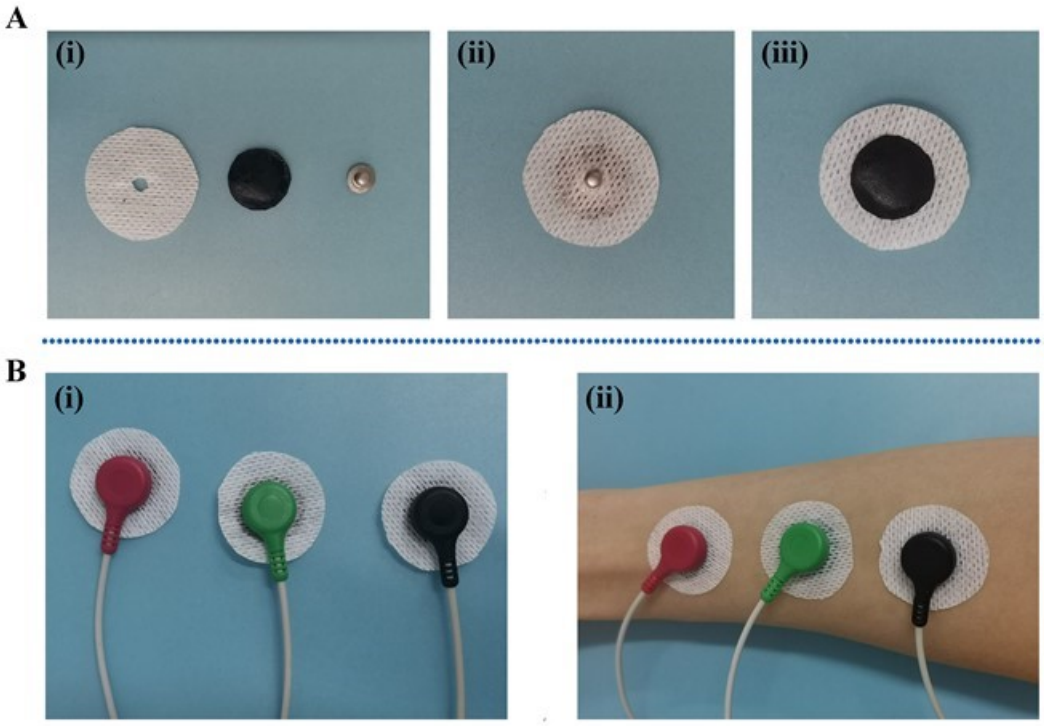

Fig. S8. (A) Manufacturing process map of GCPP-Au electrode sheet, and (B) worn on the skin surface.

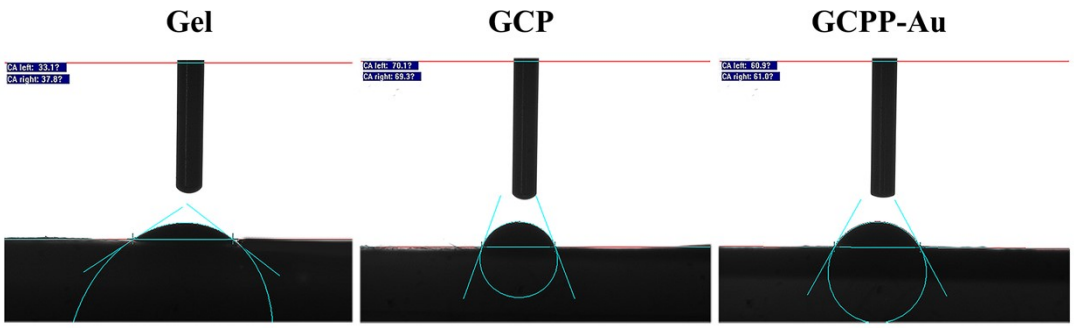

Fig. S9. Contact angle test results of Gel hydrogels, GCP and GCPP-Au flexible gel electrode materials

Note: The results showed that the pure Gel (35.45°) had good hydrophilicity, and the contact angles of GCP (69.70°) and GCPP-Au (60.95°) were lower than 90°, which was hydrophilic but relatively weak.

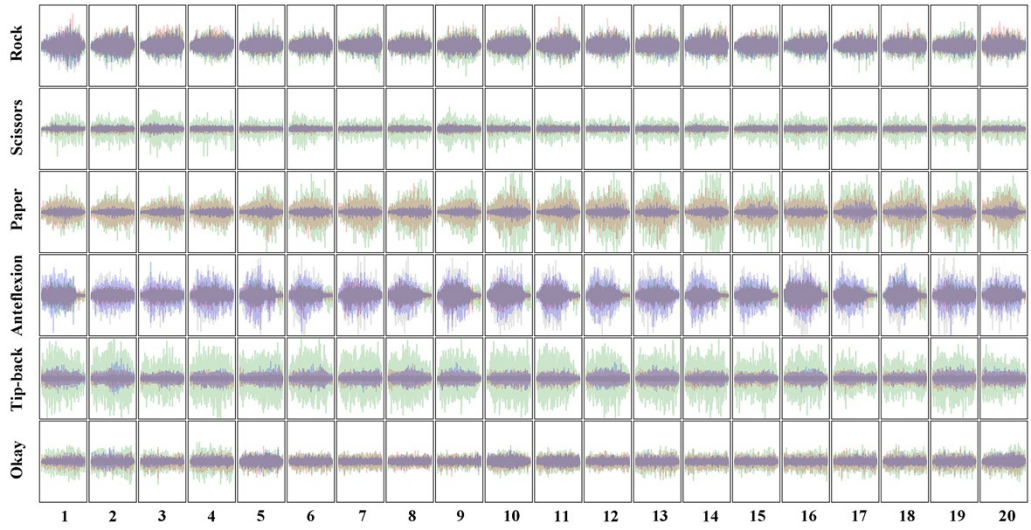

Fig. S10. 20 repetitive groups of four-channel EMG signals about different gestures

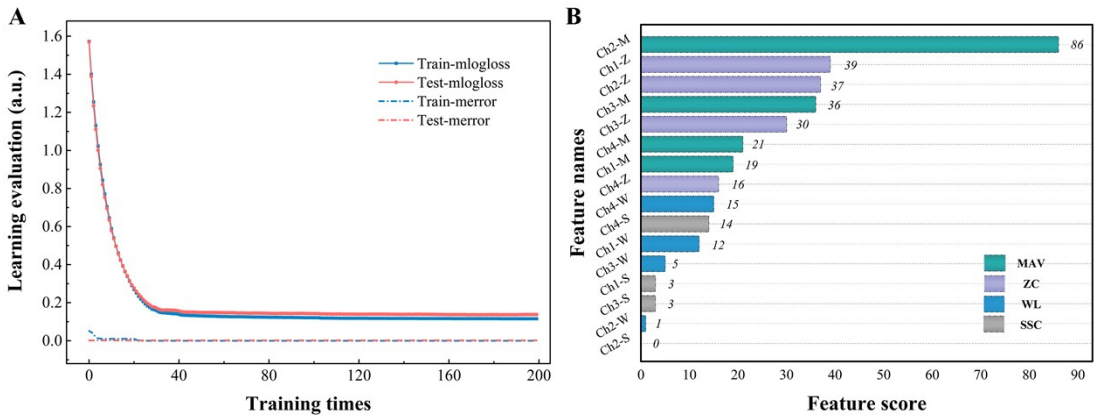

Fig. S11. Machine learning assessment, (A) train mlogloss and train merror, (B) characteristic mapping.

Eq. S1

$$\mathrm{RMS}=\sqrt{\frac{1}{\mathrm{N}}\sum_{i=1}^{\mathrm{N}}x_i^2}$$

Eq. S2

$$\mathrm{IAV}=\sum_{i=1}^{\mathrm{N}}|x_i|$$

Eq. S3

$$\mathrm{VAR}=\frac{1}{\mathrm{N}-1}\sum_{i=1}^{\mathrm{N}}x_i^2$$

Eq. S4

$$\mathrm{WAMP}=\sum_{i=1}^{N-1}\left[f(|x_n-x_{n+1}|)\right],\ f(x)=\begin{cases}1, & \text{if } x \geq \text{threshold}\\ 0, & \text{otherwise}\end{cases}$$

Eq. S5

$$\mathrm{PKF}=\max(P_j),\ j=1,\ ...,\ M.$$

where Pj is the EMG power spectrum at frequency bin j. PKF is the frequency at which the maximum power occurs.

1. Q. He, Y. Huang and S. Wang, *Advanced Functional Materials*, 2018, **28**, 1705069.